

BeppoSAX spectroscopy of the globular cluster X-ray source XB 1746-371 (NGC 6441)

A.N. Parmar¹, T. Oosterbroek¹, M. Guainazzi¹, A. Segreto², D. Dal Fiume³, and L. Stella⁴

¹ Astrophysics Division, Space Science Department of ESA, ESTEC, Postbus 299, 2200 AG Noordwijk, The Netherlands

² Istituto di Fisica Cosmica ed Applicazioni all'Informatica, CNR, Via U. La Malfa 153, 90146 Palermo, Italy

³ Istituto Tecnologie e Studio Radiazioni Extraterrestri, CNR, Via Gobetti 101, 40129 Bologna, Italy

⁴ Osservatorio Astronomico di Roma, Via Frascati 33, Monteporzio Catone, I-00040 Roma, Italy

Received ; Accepted: 1999 August 18

Abstract. During a BeppoSAX observation of the X-ray source XB 1746-371 located in the globular cluster NGC 6441 a type I X-ray burst, parts of 4 intensity dips, and energy dependent flaring were detected. The dips repeat every 5.8 ± 0.3 hr and show no obvious energy dependence. If the dips are due to electron scattering this energy independence implies an abundance > 130 times less than solar, confirming an earlier measurement. Since the overall cluster abundance is close to solar this low abundance is unexpected. Photoionization of the absorbing material, obscuration of an extended source, and variations in multiple components that combine to produce an *apparent* energy independence are all excluded. Thus, the nature of the dips remains uncertain. The best-fit model to the overall 0.3–30 keV spectrum is a disk-blackbody with a temperature of 2.82 ± 0.04 keV, together with a cutoff power-law with a photon index of -0.32 ± 0.80 and a cutoff energy of 0.90 ± 0.26 keV. Absorption, consistent with the optical extinction to NGC 6441 of $(0.28 \pm 0.04) \times 10^{22}$ atom cm $^{-2}$ is required. All previous best-fit spectral models for this source are excluded at high confidence. The spectrum is dominated by the blackbody-like component, with the cutoff power-law only contributing an average of 12% of the 1–10 keV flux. During flaring intervals the contribution of this component decreases to $\sim 6\%$ with variations in the intensity of the blackbody-like component being responsible for most of the flaring activity.

Key words: Accretion, accretion disks – Stars: XB 1746-371 – Stars: neutron – Globular cluster: NGC 6441 – X-rays: bursts – X-rays: general

1. Introduction

XB 1746-371 is one of around ten low-mass X-ray binaries (LMXRBs) known to exhibit periodic irregular dips

Send offprint requests to: A.N.Parmar (aparmar@astro.estec.esa.nl)

in X-ray intensity. These are probably caused by obscuration of the central X-ray source by material located in the thickened outer region of the accretion disk associated with the impact of the gas stream from the companion. The depth, duration and spectral properties of the dips vary from source to source, and from cycle to cycle (see Parmar & White 1988; White et al. 1995 for reviews). The study of dips provides a powerful probe of the properties of the absorbing and emitting regions in LMXRBs.

The spectral evolution during dips is complex. In most sources a cold absorber model fails to adequately represent the dip spectra which show excesses at energies $\lesssim 4$ keV. In XB 1746-371 and X 1755-338 the dips appear highly energy independent. Explanations for this energy independence include (1) an abundance, or metallicity, of the absorbing material of at least two orders of magnitude less than cosmic (White et al. 1984; Parmar et al. 1989). (2) Photoionization of the absorbing material implying that it is located well within the outer radius of the accretion disk (Frank et al. 1987). (3) Partial covering of an extended source (Sztajno & Frank 1984). (4) Variations in multiple continuum components which combine to produce an *apparent* energy independence (Church & Balucińska-Church 1993). One of the components is usually taken to be a power-law or a cutoff power-law and the other either a blackbody or a disk-blackbody.

A 12 hour duration uninterrupted EXOSAT observation of XB 1746-371 detected three apparently energy independent intensity dips separated by 5.0 ± 0.5 hr (Parmar et al. 1989). The dips have a duty cycle of $\sim 20\%$ and are not total, with $\sim 85\%$ of the 1–10 keV non-dip continuum remaining. Their periodic nature was confirmed by *Ginga* observations which refined the dip period to be 5.73 ± 0.15 hr (Sansom et al. 1993). XB 1746-371 is located within the globular cluster NGC 6441 whose properties are summarized in Layden et al. (1999). The overall cluster metallicity has been estimated to be only a factor 3 less than cosmic (Djorgovski 1993). Variations

in abundance within the cluster are expected to be at most a factor ~ 3 (e.g., Norris et al. 1981). Thus, the expected abundance of the material in XB 1746-371 differs strongly from that implied by the energy independence of the dips of >150 less than solar (Parmar et al. 1989). Two X-ray bursts were detected during the EXOSAT observation (Sztajno et al. 1987). The luminosity of these bursts is close to Eddington at the 10.7 kpc (Djorgovski 1993) distance of NGC 6441 indicating that the central neutron star is directly observed. Recently, the optical counterpart to XB 1746-371 has been detected using the Hubble Space Telescope (Deutsch et al. 1998). Its B magnitude of 18.2 implies a ratio of X-ray to optical luminosity, L_x/L_{opt} , of $\sim 10^3$ supporting the view that the central source is directly observed (see van Paradijs 1995). The counterpart exhibited $\sim 30\%$ ultraviolet variability between two exposures separated by 0.5 hr.

The EXOSAT Medium-Energy 1–15 keV non-dip spectrum of XB 1746-371 can be represented by a power-law with a photon index, α , of 2.0 and low-energy absorption, N_{H} , equivalent to 0.82×10^{22} atom cm $^{-2}$ (Parmar et al. 1989). Callanan et al. (1995) re-analyzed the EXOSAT spectrum of XB 1746-371 including a 0.04–2.0 keV measurement from a low-energy imaging telescope. They find that as well as a power-law a blackbody with a temperature, kT , of 1.08 ± 0.34 keV is required in order to obtain a satisfactory fit. The higher quality 2–17 keV *Ginga* spectrum of Sansom et al. (1993) cannot be successfully fit with any of the standard models. However, the best result is also obtained with a power-law, but with a reduced χ^2 of 4.2 with 21 degrees of freedom (dof). This suggests a complex underlying spectrum, or that the effects of energy dependent flaring observed by *Ginga* are significant. In contrast, the spectrum obtained from a short 0.5–20 keV *Einstein* Solid-State Spectrometer and Monitor Proportional Counter array observation in 1979 could be well fit by either a cutoff power-law model ($E^{-\alpha} \exp{-(E/E_{\text{co}})}$) with $\alpha = 0.96 \pm 0.01$ and $E_{\text{co}} = 6.08 \pm 0.55$ keV, or the combination of 1.89 keV blackbody and 8.3 keV bremsstrahlung components (Christian & Swank 1997).

In this *paper* we report on a broad-band observation of XB 1746-371 with BeppoSAX designed to constrain the continuum shape, investigate any spectral changes during dips, and quantify the time variability of the source.

2. Observations

Results from the Low-Energy Concentrator Spectrometer (LECS; 0.1–10 keV; Parmar et al. 1997), the Medium-Energy Concentrator Spectrometer (MECS; 1.8–10 keV; Boella et al. 1997), the High Pressure Gas Scintillation Proportional Counter (HPGSPC; 5–120 keV; Manzo et al. 1997) and the Phoswich Detection System (PDS; 15–300 keV; Frontera et al. 1997) on-board BeppoSAX are presented. All these instruments are coaligned

and collectively referred to as the Narrow Field Instruments, or NFI. The MECS consists of two grazing incidence telescopes with imaging gas scintillation proportional counters in their focal planes. The LECS uses an identical concentrator system as the MECS, but utilizes an ultra-thin entrance window and a driftless configuration to extend the low-energy response to 0.1 keV. The non-imaging HPGSPC consists of a single unit with a collimator that remained on-source during the entire observation. The non-imaging PDS consists of four independent units arranged in pairs each having a separate collimator. Each collimator was alternatively rocked on- and off-source during the observation.

The region of sky containing XB 1746-371 was observed by BeppoSAX on 1999 April 04 18:07 UT to April 05 20:23 UT. Good data were selected from intervals when the elevation angle above the Earth's limb was $>4^\circ$ and when the instrument configurations were nominal, using the SAXDAS 2.0.0 data analysis package. The standard PDS collimator dwell time of 96 s for each on- and off-source position was used together with a rocking angle of $210'$. LECS and MECS data were extracted centered on the position of XB 1746-371 using radii of $8'$ and $4'$, respectively. The exposures in the LECS, MECS, HPGSPC, and PDS instruments are 16.3 ks, 49.9 ks, 48.7 ks, and 23.3 ks, respectively. Background subtraction for the imaging instruments was performed using standard files, but is not critical for such a bright source. Background subtraction for the HPGSPC was carried out using data obtained when the instrument was looking at the dark Earth and for the PDS using data obtained during intervals when the collimator was offset from the source.

3. Results

3.1. X-ray Lightcurve

Fig. 1 shows the 1.8–10 keV MECS lightcurve of XB 1746-371 with a binning of 512 s. Substantial intensity variability is present as well as an X-ray burst, which is strongly truncated due to the long binning. If the X-ray burst is ignored, the average root mean square variability of the 256 s binned light curve is $7.8 \pm 0.4\%$. The flaring activity and burst are not strongly evident in the 15–30 keV PDS lightcurve due to the low count rate in this instrument.

The dipping activity seen by EXOSAT and *Ginga* is not readily apparent in Fig. 1. To investigate whether dipping is in fact present during the BeppoSAX observation a Fast Fourier Transform (FFT) of the 1.8–10 keV MECS data excluding the bursting interval was computed. This was rebinned in a logarithmic fashion. Fig. 2 shows the FFT between 10^{-5} and 10^{-3} Hz. A “spike” is visible at around 5×10^{-5} Hz, together with a large excess of power at frequencies $< 3 \times 10^{-5}$ Hz, and a smaller feature at $\sim 2 \times 10^{-4}$ Hz, corresponding to the BeppoSAX orbital frequency. The 5×10^{-5} Hz “spike” is at a fre-

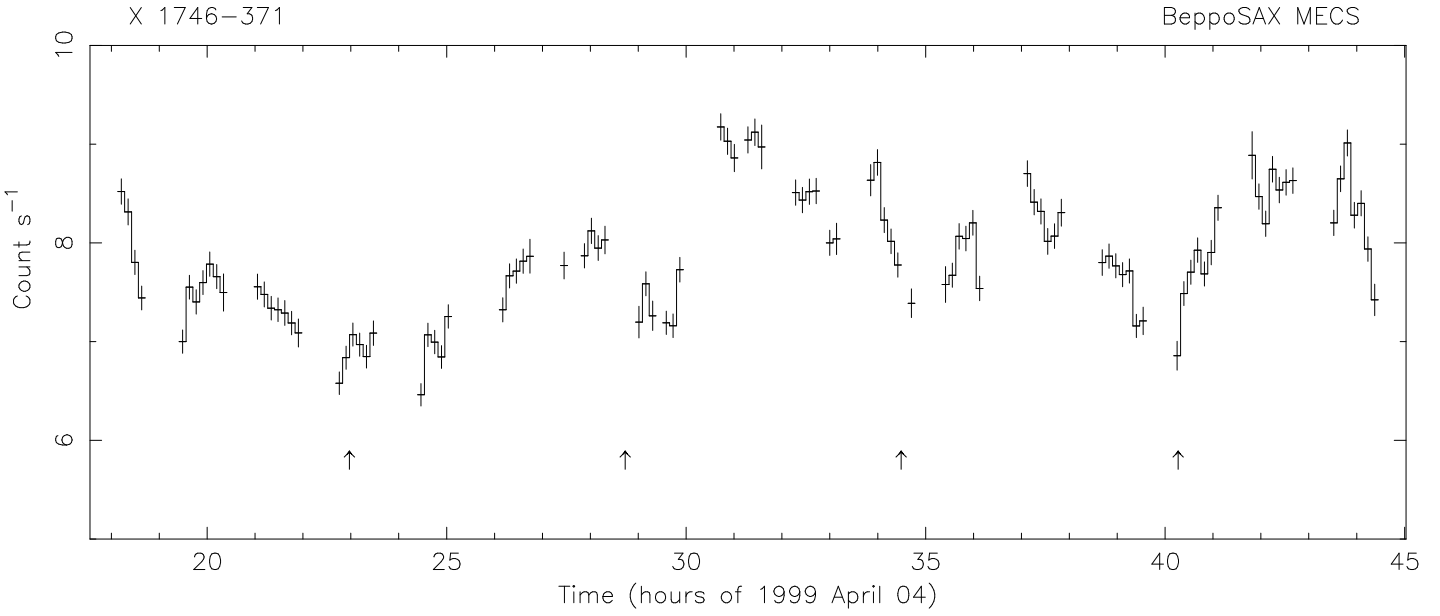


Fig. 1. MECS 1.8–10 keV lightcurve of XB 1746-371 with a binning of 512 s. The X-ray burst that occurs at around 44 hrs is strongly truncated by the binning. The arrows indicate the times of minima of the folded lightcurve

frequency consistent with the dipping activity seen by EXOSAT and *Ginga*. This implies that similar dipping activity is present during the BeppoSAX observation. In order to compare this variability with that seen earlier, a 1.8–10 keV lightcurve with a 4096 s binning was produced and a 3rd order polynomial fit to these data. A 256 s integration lightcurve was then divided by the 3rd order polynomial in order to reduce the effects of long-term variability. The dip recurrence interval was then determined to be 5.8 ± 0.3 hr by epoch folding. This value is consistent with the period derived from the *Ginga* observation of 5.73 ± 0.15 hr (Sansom et al. 1993). The minimum of the BeppoSAX folded lightcurve occurs at MJD 51273.20 ± 0.02 .

The variation in spectral hardness with count rate was next investigated. The hardness ratio is defined as the count rate in the energy range 4.0–10.0 keV divided by that in the range 1.8–4.0 keV. Fig. 3 shows the MECS hardness ratio plotted against 1.8–10 keV count rate with a binning time of 512 s. The hardness ratio clearly increases with increasing count rate with a probable flattening at lower count rates. If intervals with 1.8–10 keV MECS count rate >7.5 s $^{-1}$ are selected, then the hardness ratio gradient is 0.075 ± 0.008 count $^{-1}$ s (90% confidence). Similarly, if intervals with count rates below this value are selected, then the hardness ratio gradient is 0.049 ± 0.027 count $^{-1}$ s. Similar trends are evident in the *Ginga* data reported in Sansom et al. (1993). The low-count rate intervals tend to be associated with dipping activity, and the small change in hardness ratio at low count rates confirms the presence of the (almost) energy-independent dipping discovered with EXOSAT (Parmar et al. 1989).

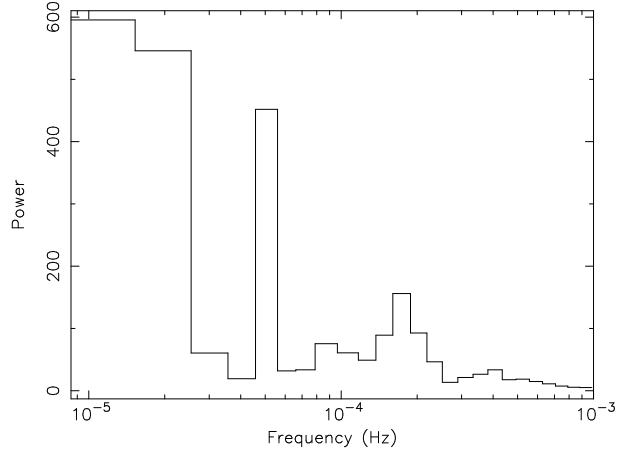


Fig. 2. The XB 1746-371 1.8–10 keV MECS FFT. Power is in units of “Leahy” power. The “spike” at around 5×10^{-5} Hz corresponds to the dipping activity. The peak at $\sim 2 \times 10^{-4}$ Hz is consistent with the BeppoSAX orbital frequency

Fig. 4 shows the 1.8–10 keV MECS lightcurve folded on the best-fit dip period given above. The interval corresponding to the X-ray burst has been excluded and the data divided by the best-fit 3rd-order polynomial. The peak-to-peak variability of the folded lightcurve is $14 \pm 1\%$. With the exception of the large peak at phase ~ 0.3 , the BeppoSAX folded lightcurve is similar to those of Sansom et al. (1993). This similarity provides further support for the presence of dips during the BeppoSAX observation. Examination of Fig. 1 reveals that the high count rate at ~ 31 hrs contributes significantly to the peak in the folded lightcurve, but that similar intensity maxima are

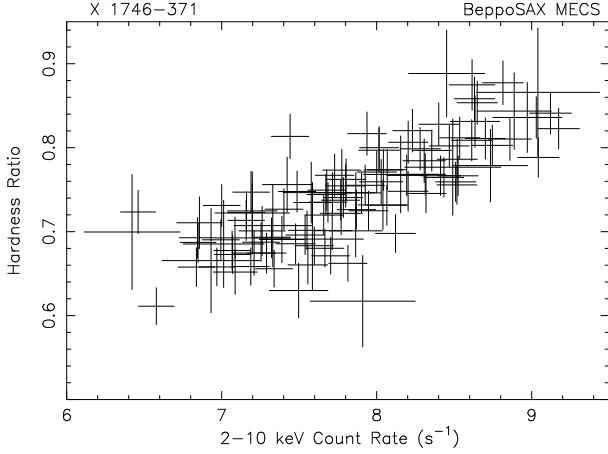


Fig. 3. The XB 1746-371 MECS hardness ratio plotted against 1.8–10 keV count rate. The hardness ratio increases with increasing count rate and shows a tendency to flatten at the lowest count rates

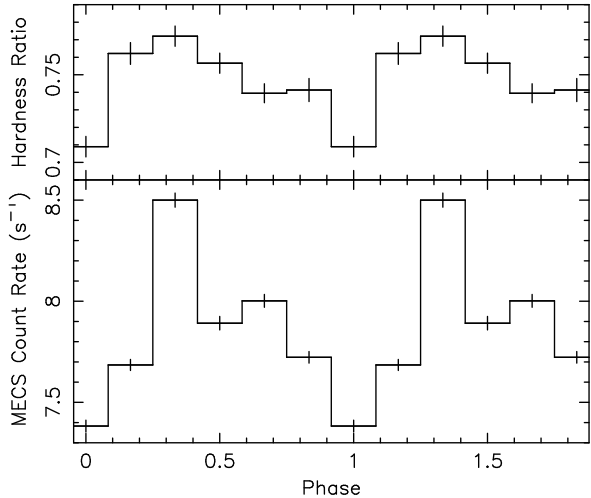


Fig. 4. The XB 1746-371 1.8–10 keV MECS lightcurve (lower panel) and hardness ratio (upper panel) folded over the 5.8 hr dip period, after removal of the long-term variability and normalized to the mean count rate. The interval corresponding to the X-ray burst is excluded

not seen during the other 4 phase 0.3 intervals observed. This suggests that the peak at phase ~ 0.3 in the folded lightcurve results from intrinsic variability, rather than an orbital modulation. Given the sharpness of the lightcurve and hardness ratio minima, Fig. 4 suggests that dipping activity probably occurs over $\sim 15\%$ of the orbital cycle.

3.2. Overall Spectrum

The overall spectrum of XB 1746-371 was first investigated by simultaneously fitting data from all the BeppoSAX NFI. The interval corresponding to the burst was excluded. The LECS and MECS spectra were rebinned to oversample the full width half maximum of the energy res-

olution by a factor 3 and to have additionally a minimum of 20 counts per bin to allow use of the χ^2 statistic. The HPGSPC and PDS spectra were rebinned using the standard techniques in SAXDAS. Data were selected in the energy ranges 0.3–4.0 keV (LECS), 1.8–10 keV (MECS), 8.0–20 keV (HPGSPC), and 15–30 keV (PDS) where the instrument responses are well determined and sufficient counts obtained. This gives background-subtracted count rates of 2.9, 7.8, 3.3 and 0.8 s^{-1} for the LECS, MECS, HPGSPC, and PDS, respectively. The photoelectric absorption cross sections of Morisson & McCammon (1983) and the solar abundances of Anders & Grevesse (1989) are used throughout

Initially, simple models were tried, including absorbed power-law, thermal bremsstrahlung and cutoff power-law models. Factors were included in the spectral fitting to allow for normalization uncertainties between the instruments. These factors were constrained to be within their usual ranges during the fitting. A power-law with $\alpha = 2.2$ and a 8.6 keV bremsstrahlung give unacceptable fits with χ^2 's of 16000 and 3000 for 110 dof, respectively. A cutoff power-law model with $\alpha = 0.74$ and $E_{\text{co}} = 4.9$ keV gives a better fit with a χ^2 of 370 for 109 dof. Next more complex models consisting of a bremsstrahlung and a blackbody and a power-law and a disk-blackbody (Mitsuda et al. 1984; Makishima et al. 1986) were tried for comparison with previous results. The disk-blackbody model assumes that the gravitational energy released by the accreting material is locally dissipated into blackbody radiation, that the accretion flow is continuous throughout the disk, and that the effects of electron scattering are negligible. There are only two parameters of the model, $r_{\text{in}}(\cos i)^{0.5}$ where r_{in} is the innermost radius of the disk, i is the inclination angle of the disk and kT_{BB} the blackbody effective temperature at r_{in} . Both these models gave somewhat better fits with χ^2 's of 180.3 and 179.3 for 108 dof.

Inspection of the residuals of the power-law and disk-blackbody fit suggests that the power-law should be replaced by a cutoff power-law. This results in an acceptable χ^2 of 108.0 for 107 dof. If the disk-blackbody is replaced by a 0.50 keV blackbody, the fit is still acceptable with a χ^2 of 112.3 for 107 dof. An F-test indicates that the probability of chance improvement is 87%. The blackbody radius is 12.5 ± 0.3 km and $r_{\text{in}}(\cos i)^{0.5}$ from the disk-blackbody fit is 1.03 ± 0.11 km, both for a distance of 10.7 kpc. Since i is likely to be $\approx 70^\circ$ (see Sect. 4) the disk-blackbody fit implies an unusually small emitting region of ≈ 2 km radius. The fit results are summarized in Table 1 and the fit using the cutoff power-law and disk-blackbody model is shown in Fig. 5. The overall 1–10 keV flux is $8.6 \times 10^{-10} \text{ erg cm}^{-2} \text{ s}^{-1}$, which corresponds to a luminosity of $1.2 \times 10^{37} \text{ erg s}^{-1}$ at a distance of 10.7 kpc. The cutoff power-law is much weaker than the disk-blackbody (or blackbody), only contributing 12% (11%) of the 1–10 keV luminosity, and with a maximum

Table 1. XB 1746-371 overall spectral fit results. N_{H} is in units of 10^{22} atom cm $^{-2}$. $r_{\text{in}}(\cos i)^{0.5}$ is in units of km for a distance of 10.7 kpc. 90% confidence limits are given. PL = power-law, DBB = disk-blackbody

Model	N_{H}	kT (keV)	kT_{BB} (keV)	α	E_{co} (keV)	$r_{\text{in}}(\cos i)^{0.5}$	χ^2/dof
Bremss + blackbody	0.44 ± 0.015	6.39 ± 0.20	1.85 ± 0.04	180.3/108
PL + DBB	0.53 ± 0.03	...	2.68 ± 0.03	2.59 ± 0.09	...	1.15 ± 0.05	179.3/108
Cutoff PL + blackbody	0.21 ± 0.02	...	0.50 ± 0.02	0.18 ± 0.04	3.5 ± 0.7	...	112.3/107
Cutoff PL + DBB	0.28 ± 0.04	...	2.82 ± 0.04	-0.32 ± 0.80	0.90 ± 0.26	1.03 ± 0.11	108.0/107

contribution around 1 keV (see Fig. 5). Since this component is so weak its overall shape is poorly constrained and if it is replaced by e.g. a 3.5 keV thermal bremsstrahlung the resulting χ^2 is 126.4 for 108 dof. Similarly, replacing it by a 0.55 keV blackbody gives a χ^2 of 114.9 for 108 dof, marginally worse than the cutoff power-law and blackbody fit. However, replacing the faint component with the COMPTT model in XSPEC, used to describe the Comptonization of cool photons in a hot plasma, does not give an acceptable fit. The 90% confidence upper limit to the equivalent width of a narrow Fe line at 6.5 keV is 15 eV. Absorption equivalent to $(0.28 \pm 0.04) \times 10^{22}$ atom cm $^{-2}$ is required. The optical extinction to NGC 6441, A_v , is 1.30 magnitudes (Djorgovski 1993) which corresponds to an N_{H} of 0.23×10^{22} atom cm $^{-2}$ using the relation in Predehl & Schmitt (1995). Thus, there is no strong evidence for significant absorption intrinsic to the X-ray source.

3.3. Intensity Selected Spectra

Fig. 3 illustrates that the hardness ratio depends on intensity. In order to investigate the energy dependence of this variability, a series of intensity selected spectra were produced. Intervals corresponding to MECS 1.8–10 keV count rates of <7.2 , 7.2–7.6, 7.6–8.1, 8.1–8.6, >8.6 s $^{-1}$, before any long-term trend removal when the data are accumulated with a binning of 256 s, were determined. These intervals were used to extract a set of corresponding 5 NFI spectra which were then rebinned and energy selected in the same way as in Sect. 3.2. Since the cutoff power-law and disk-blackbody model provides the best fit to the overall spectrum, this model was also fit to these new spectra.

The fit results are given in Table 2. With the exception of the lowest intensity selection, the spectra are well fit by the model. Examination of the residuals of the lowest intensity fit shows that there are no obvious systematic deviations between model and data, and that the data just appear to be “noisy”. Allowing different amounts of low-energy absorption for the two components does not produce a significant improvement in fit quality. If the minimum absorption of the cutoff power-law is constrained to be equal to the interstellar value of 0.23×10^{22} atom cm $^{-2}$ (see Sect. 3.2), the 90% confidence

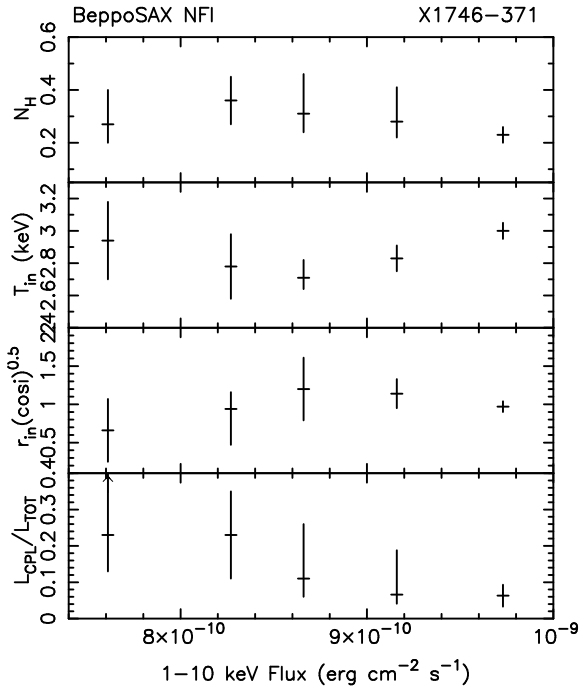


Fig. 6. The dependence of N_{H} , T_{in} , $r_{\text{in}}(\cos i)^{0.5}$ and the ratio of 1–10 keV fluxes in the cutoff power-law and disk-blackbody components against intensity. The units are the same as in Table 2

limit to any additional absorption on the disk-blackbody is 0.48×10^{22} atom cm $^{-2}$. The best-fit values of N_{H} , T_{in} , $r_{\text{in}}(\cos i)^{0.5}$ and the ratio of 1–10 keV fluxes in the cutoff power-law compared to the total are shown plotted against total 1–10 keV flux in Fig. 6. There is no systematic change in N_{H} with intensity. The values of T_{in} and $r_{\text{in}}(\cos i)^{0.5}$ are strongly correlated and have no obvious luminosity dependence. The spectral parameters of the cutoff power-law are not well determined and are also strongly correlated, and so we consider only the intensity dependence of the luminosity of this component. Table 2 and Fig. 6 show that the contribution of the cutoff power-law to the total decreases from $\sim 23\%$ at a flux of 7.6×10^{-10} erg cm $^{-2}$ s $^{-1}$ keV $^{-1}$ to $\sim 6\%$ at a flux of 9.7×10^{-10} erg cm $^{-2}$ s $^{-1}$ keV $^{-1}$. This means that the intensity of the cutoff power-law decreased by a factor ~ 3 as the overall intensity increased by 28% and that the majority of the flaring activity may be mod-

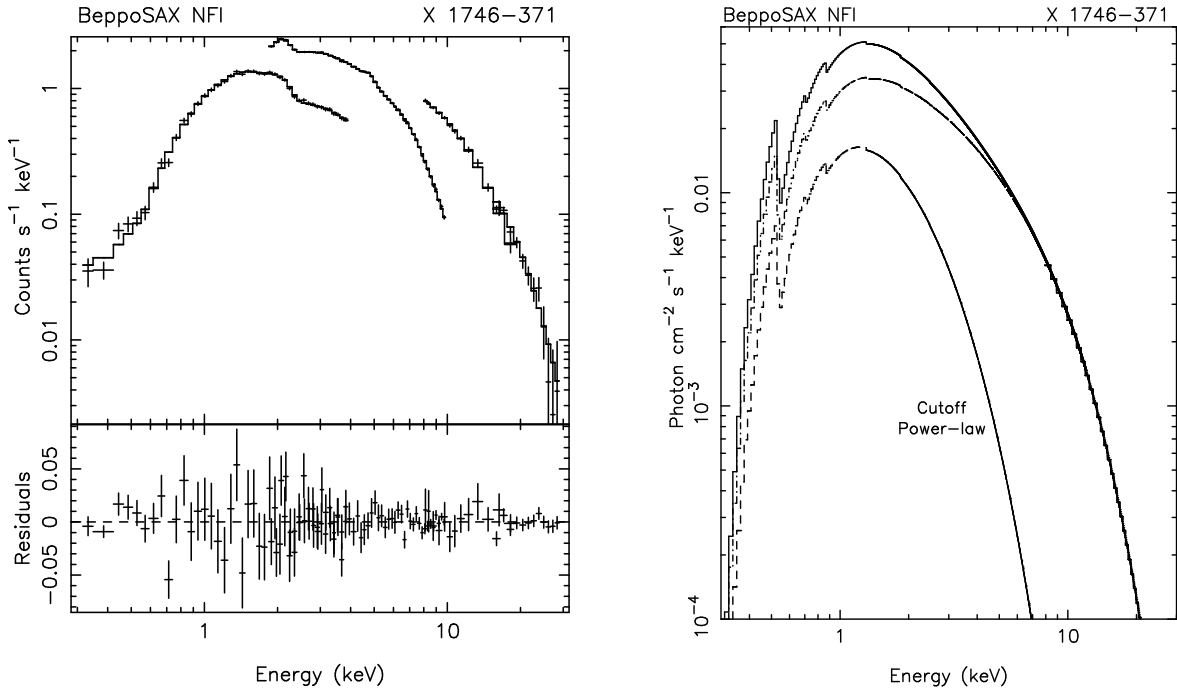


Fig. 5. The overall XB 1746-371 NFI spectrum together with the best-fit cutoff power-law and disk-blackbody model fit (see Table 1). The lower-left panel shows the fit residuals in units of counts $\text{s}^{-1} \text{ keV}^{-1}$. The right panel shows the assumed photon spectrum with the contributions of the cutoff power-law and disk-blackbody components indicated separately

eled by changes in the intensity of the disk-blackbody. A similar result is obtained if the disk-blackbody is substituted by a blackbody.

3.4. Dip Spectrum

In order to investigate the spectral behavior during dips an NFI spectrum corresponding to the lowest bin of the folded lightcurve (Fig. 4) was extracted. This covers phases 0.92–1.08 of the ephemeris given in Sect. 3.1. This selection was chosen since both the folded lightcurve and hardness ratios (Fig. 4; upper panel) show large differences between this and adjacent bins. This suggests that the dipping activity occurs primarily within this single phase bin. The spectrum was rebinned and energy selected in the same way as in Sect. 3.2. The resulting exposure times are 2.3 ks, 8.2 ks, 7.6 ks, 3.7 ks for the LECS, MECS, HPGSPC, and PDS, respectively.

Since dips are believed to be due to obscuration of the central X-ray source by intervening material, the usual method of analyzing the spectral changes during dipping activity is to fix the spectral shape to that outside of dips and only allow the amount of absorption and/or scattering to vary (e.g., Parmar et al. 1986; Church et al. 1998). In the case of XB 1746-371, this procedure is likely to give incorrect results since the non-dip spectral shape depends on luminosity (see Fig. 3) and it is not possible to easily separate intrinsic variability from dipping ac-

tivity. Instead, the cutoff power-law and disk-blackbody model was fit to the NFI dip spectrum with all the parameters free, as before. The resulting χ^2 is 117.5 for 102 dof. Unsurprisingly, the best-fit parameter values are consistent with those obtained for the lowest ($<7.5 \text{ count s}^{-1}$) intensity selected interval. The best-fit value of N_{H} is $(0.25 \pm 0.09) \times 10^{22} \text{ atom cm}^{-2}$ which implies that any change in N_{H} during the dips is $\lesssim 0.06 \times 10^{22} \text{ atom cm}^{-2}$, when compared to the overall value. For comparison, the column of electrons required to produce the observed mean reduction in flux during the dips of 5% by scattering is $8 \times 10^{22} \text{ cm}^{-2}$. This difference implies an abundance anomaly of >130 less than solar, comparable with the EXOSAT value of >150 less than solar (Parmar et al. 1989), which was obtained with the spectral parameters held fixed.

4. Discussion

We have observed XB 1746-371 in the 0.3–30 keV energy range using BeppoSAX. Although the dipping activity observed by EXOSAT and *Ginga* is not readily apparent in the BeppoSAX lightcurve, an FFT of the 1.8–10 keV MECS data reveals evidence for excess variability on a timescale of ~ 5 hr. A folding analysis gives a best period of 5.8 ± 0.3 hr, consistent with earlier EXOSAT and *Ginga* measurements. When the effects of intrinsic variability are ignored, the folded lightcurve is similar to those observed by *Ginga*. The above similarities imply that dipping is

Table 2. XB 1746-371 intensity selected NFI spectral fit results using the disk-blackbody and cutoff power-law model. N_{H} is in units of 10^{22} atom cm^{-2} . $r_{\text{in}}(\cos i)^{0.5}$ is in units of km for a distance of 10.7 kpc. $L_{\text{CPL}}/L_{\text{TOT}}$ is the 1–10 keV ratio of the cutoff power-law to the total luminosity. 90% confidence limits are given

Parameter	MECS Count Rate (s^{-1})				
	<7.2	7.2–7.6	7.6–8.1	8.1–8.6	>8.6
MECS Exp. (ks)	7.9	10.0	14.0	10.2	7.0
N_{H}	0.27 ± 0.07	0.36 ± 0.09	0.31 ± 0.07	0.28 ± 0.06	0.23 ± 0.03
α	0.25 ± 1.20	0.70 ± 1.5	0.0 ± 2.0	-0.40 ± 2.5	-3.0 ± 1.6
E_{co} (keV)	1.4 ± 0.7	1.7 ± 6.0	1.0 ± 4.5	0.8 ± 2.7	0.41 ± 0.03
T_{in} (keV)	2.94 ± 0.24	2.78 ± 0.20	2.71 ± 0.11	2.83 ± 0.08	3.00 ± 0.05
$r_{\text{in}}(\cos i)^{0.5}$	0.66 ± 0.41	0.94 ± 0.47	1.20 ± 0.41	1.14 ± 0.19	0.97 ± 0.07
$L_{\text{CPL}}/L_{\text{TOT}}$	0.23 ± 0.10	0.23 ± 0.12	0.11 ± 0.05	0.066 ± 0.025	0.063 ± 0.003
χ^2/dof	122.3/103	100.2/103	109.1/104	94.3/104	106.7/104

present during the BeppoSAX observation. Examination of the EXOSAT and *Ginga* lightcurves reveals that it is unsurprising that the dips are so hard to see in the BeppoSAX data. This is because the *Ginga* mean count rate is $\sim 190 \text{ s}^{-1}$, compared to 7.8 count s^{-1} for the MECS, while the continuous observation of EXOSAT confers an obvious advantage.

The 0.3–30 keV XB 1746-371 spectrum is clearly complex and requires at least two continuum components. The best-fit model for the overall spectrum consists of a disk-blackbody together with a cutoff power-law. However, we cannot exclude that the soft component is actually a blackbody, rather than a disk-blackbody, or that the cutoff power-law actually has another form. A better resolution of this spectral complexity awaits further studies. In contrast to e.g., the dip source X 1916-053 which was detected to energies of $\gtrsim 100$ keV by BeppoSAX and where the thermal component contributes 20% of the 1–10 keV flux (Church et al. 1998), the XB 1746-371 spectrum is dominated by the thermal component resulting in the source being only detected to ~ 30 keV. The source becomes harder during flaring intervals, confirming the *Ginga* result of Sansom et al. (1993). Changes in the disk-blackbody component are responsible for most of the flaring activity. During flares the intensity of the cutoff power-law component decreases.

We can exclude at high confidence the best-fit models obtained using EXOSAT (PL, or cutoff PL; Parmar et al. 1989, PL + blackbody; Callanan et al. 1995), *Ginga* (PL; Sansom et al. 1993) and *Einstei*n (cutoff PL, or bremsstrahlung and blackbody; Christian & Swank 1997). However, it is possible that we are observing XB 1746-371 in an unusual state and at other times the spectrum could be represented by a more simple model. Some support for this idea comes from the HEAO-1 A4 catalog where XB 1746-371 is detected in the 40–80 keV energy range, but with a similar overall X-ray level as during the BeppoSAX observation (Levine et al. 1984). In a survey of the hard X-ray

properties of LMXRBs using results from the A4 catalog, van Paradijs & van der Klis (1994) show that the high-energy spectra of LMXRB become softer with increasing luminosity, and that the properties of XB 1746-371 appear typical of systems with similar luminosity. It has been noted that at luminosities 10^{36} – 10^{37} erg s^{-1} the spectra of burst sources evolve from hard power-law (-like) to softer exponential (-like) shapes (White et al. 1988; Barret & Vedrenne 1994).

In general, the spectra of LMXRB are interpreted in terms of an accretion disk around a weakly magnetized neutron star. This gives rise to two spectral components (e.g., White et al. 1988; Barret & Vedrenne 1994). A “thermal-like” component represents the emission from an optically thick region such as the neutron star surface (Mitsuda et al. 1984) or a boundary layer between the accretion disk and the neutron star surface (White et al. 1988). The second component is often represented by a cutoff power-law which is an approximation of the spectral shape expected from the Comptonization of cool photons on hot electrons. Based on the spectral changes during dips, where the blackbody-like component is obscured more rapidly and deeply than the Comptonized component (e.g., Church et al. 1998), and the discovery of hard X-ray time lags (e.g., Ford et al. 1999), this component is almost certainly extended in a number of sources. There are at least two possible explanations as to why the Comptonized component is so weak in XB 1746-371. (1) It is possible that the luminosity of XB 1746-371 is close to the “critical” value where the spectra of LMXRBs may change from a power-law (-like) to an exponential (-like) form. If this is so, a small change in the accretion rate may produce a large change in spectral shape. (2) The geometry of XB 1746-371 may be somehow different from the majority of LMXRBs. In particular, due to the inclination angle through which the system is viewed (see below) it may be possible that a significant fraction of an extended Comptonizing region is hidden behind the accretion disk. This could occur if e.g. a relatively small Comptonizing

region surrounds the neutron star and is partly obscured by the flared inner regions of the accretion disk.

The orbital parameters of XB 1746-371 can be estimated assuming that the system contains a compact object of mass $1.4M_{\odot}$, that the orbital period is 5.73 hr and that the companion is a low-mass zero-age main-sequence star filling its Roche lobe. In this case the relation between orbital period in hours, P_{hr} , and companion mass, M_c , is $M_c \simeq 0.11 P_{\text{hr}}$. For the XB 1746-371 system this implies $M_c \simeq 0.65 M_{\odot}$. The separation between the X-ray source and its companion is $\sim 1.5 \times 10^{11}$ cm. If the accretion disk fills 70% of its Roche lobe then its radius is $\sim 7 \times 10^{10}$ cm. The absence of X-ray eclipses implies that the line of sight is inclined by $\gtrsim 20^\circ$ from the orbital plane. Similarly, the dipping behavior requires that there is structure in the accretion disk located $\gtrsim 20^\circ$ from the orbital plane.

The dipping behavior observed from XB 1746-371 is complex and poorly understood. During dips the change in low-energy absorption is $\lesssim 0.06 \times 10^{22}$ atom cm $^{-2}$ which implies an abundance of > 130 less than solar, consistent with the previous EXOSAT estimate (Parmar et al. 1989) and the non-detection of an Fe line in the X-ray spectrum. However, since the overall cluster metallicity is only a factor 3 less than solar (Djorgovski 1993), it is difficult to understand how the metallicity of the absorbing material in XB 1746-371 could be so low. The other mechanisms that could produce energy independent dips discussed in Sect. 1 can also be excluded. Photoionization of the elements responsible for photoelectric absorption in the X-ray band is unlikely to be a viable mechanism unless the material is located very close to the neutron star. Following arguments presented in Mason et al. (1985) for X 1755-338, only material within $\sim 10^{10}$ cm of the central X-ray source in XB 1746-371 is likely to fully ionized, whereas the radius of the accretion disk is expected to be $\sim 7 \times 10^{10}$ cm. Partial obscuration of an extended source is unlikely to be applicable given the high L_x/L_{opt} ratio of the system which implies that the neutron star is directly observed.

In the case of X 1755-338, where the energy independence of the dips implies an abundance > 600 times less than solar (White et al. 1984), a two component model consisting of a blackbody and a power-law which combine in such a way to produce the *apparent* energy independence, although the dips are caused (primarily) by absorption of the blackbody component, has been successfully applied (Church & Bałucińska-Church 1993). Different amounts of absorption might be expected from a point-like source located close to the center of the accretion disk and an extended (Comptonized) region. When the two component model is fit to the dip spectrum there is no evidence for significant extra absorption of the disk-blackbody component. This implies that the multiple component model used to describe the X 1755-338 dips in terms of absorption by material with solar abundance is not applicable here. Thus the nature of the dips and the

reason for their apparent energy independence remains uncertain.

Acknowledgements. The BeppoSAX satellite is a joint Italian-Dutch programme. We thank the staffs of the BeppoSAX Science Data and Operations Control Centers for help with these observations. M. Guainazzi acknowledges an ESA Fellowship.

References

Anders E., Grevesse N., 1989, *Geochimica et Cosmochimica Acta* 53, 197
 Barret D., Vedrenne G., 1994, *ApJS* 92, 505
 Boella G., Chiappetti L., Conti G., et al., 1997, *A&AS* 122, 327
 Callanan P.J., Penny A.J., Charles P.A., 1995, *MNRAS* 273, 201
 Church M., Bałucińska-Church M., 1993, *MNRAS* 260, 59
 Church M., Parmar A.N., Bałucińska-Church M., et al., 1998, *A&A* 338, 556
 Christian D.J., Swank J.H., 1997, *ApJS* 109, 177
 Deutsch E.W., Anderson S.F., Margon B., Downes R.A., 1998, *ApJ* 493, 775
 Djorgovski S., 1993, In: Djorgovski S., Meylen G., (eds.) *ASP conf. ser. 50, Structure and Dynamics of Globular Clusters*. ASP, San Francisco, p. 373
 Ford E.C., van der Klis M., Mendez M., van Paradijs J., Kaaret P., 1999, *ApJ* 512, L31
 Frank J., King A., Lasota J.-P., 1987, *A&A* 178, 137
 Frontera F., Costa E., Dal Fiume D., et al., 1997, *A&AS* 122, 371
 Layden A.C., Ritter L.A., Welch D.L., Webb T.M.A., 1999, *AJ* 117, 1313
 Levine A.M., Lang F.W., Lewin W.H.G., et al., 1984, *ApJS* 54, 581
 Makishima K., Maejima Y., Mitsuda K., et al., 1986, *ApJ* 285, 712
 Manzo G., Guarusso S., Santangelo A., et al., 1997, *A&AS* 122, 341
 Mason K.O., Parmar A.N., White N.E., 1985, *MNRAS* 216, 1033
 Mitsuda K., Inoue H., Koyama K., et al., 1984, *PASJ* 36, 741
 Morisson D., McCammon D., 1983, *ApJ* 270, 119
 Norris J., Cottrell P.L., Freeman K.C., da Costa G.S., 1981, *ApJ* 244, 205
 Parmar A.N., White N.E., 1988, *Mem. Soc. Astron. Ital.* 59, 147
 Parmar A.N., White N.E., Giommi P., Gottwald M., 1986, *ApJ* 308, 199
 Parmar A.N., Stella L., Giommi P., 1989, *A&A* 222 96
 Parmar A.N., Martin D.D.E., Baudaz M., et al., 1997, *A&AS* 122, 309
 Predehl P., Schmitt J.H.M.M., 1995, *A&A* 293, 889
 Sansom A., Dotani T., Asai K., Lehto H.J., 1993, *MNRAS* 262, 429
 Sztajno M., Frank J., 1984, *A&A* 138, L15
 Sztajno M., Fujimoto M., van Paradijs J., et al., 1987, *MNRAS* 236, 39
 Van Paradijs J., 1995, In: Lewin W.H.G., van Paradijs J., van den Heuvel E.P.J., (eds.) *X-ray Binaries*. Cambridge University Press, Cambridge, p. 536

Van Paradijs J., van der Klis M., 1994, A&A 281, L17
White N.E., Parmar A.N., Sztajno M., et al., 1984, ApJ 283,
L9
White N.E., Stella L., Parmar A.N., 1988, ApJ 324, 378
White N.E., Nagase F., Parmar A.N., 1995, In: Lewin W.H.G.,
van Paradijs J., van den Heuvel E.P.J., (eds.) X-ray Binaries.
Cambridge University Press, Cambridge, p. 1